

MODELING OF DAMAGE AND LIFETIME ANALYSIS OF PLASMA FACING COMPONENTS DURING PLASMA INSTABILITIES IN TOKAMAKS

F. Genco and A. Hassanein

Center for Materials under Extreme Environment, School of Nuclear Engineering, Purdue University, West Lafayette, IN 47907, USA

Email: fgenco@purdue.edu (F. Genco), hassanein@purdue.edu (A. Hassanein)

Off normal operating conditions resulting from plasma instabilities such as disruptions, edge-localized modes (ELM), and vertical displacement events (VDE) in tokamaks are to be expected with the potential of high energy deposition on plasma facing components (PFC). This high-energy dump in short duration, will result in extremely high temperatures of the PFC leading to melting and evaporation of the surfaces. Erosion resulting from these processes is life-limiting for the PFC as well as potential plasma contamination and degradation of performance. A comprehensive understanding based on the interplay of all physical processes during plasma instabilities on the divertor plate is necessary in order to improve reliability and characterize the performance of this key component. A novel particle-in-cell (PIC) technique has been developed and integrated into the existing HEIGHTS package in order to verify and have another perspective in assessing these problems.

The HEIGHTS multi-dimensional integrated models take into account different stages of the plasma material interaction and its evolution along time. The extent of the damage will essentially depend on the intensity and duration of energy deposited on PFC. Both bulk and surface damages can take place depending on these parameters. For this reason different deposition times have been considered ranging from several microseconds to tens of milliseconds in order to provide comprehensive evolution of material erosion and transport. Comparison of the newly implemented PIC methods with current HEIGHTS existing models are discussed.

I. INTRODUCTION

Damage to plasma facing components (PFCs) as consequence of plasma instabilities in tokamak reactors still represents the biggest obstacle to their successful development as energy producing reactors. Loss of confinement and instabilities as edge localized modes (ELMs) and vertical displacements events (VDE), can lead to major hard disruptions that can include both thermal and current quench. These intense energy deposition events ($10 - 200 \text{ MJ} / \text{m}^2$) over very short times (0.1-500 ms) may result in severe surface and bulk

damage to both plasma-facing and structural materials^{1,2}. The degradation of performance of PFC is extremely enhanced during off-normal events since the large heat fluxes involved provoke large temperature gradients, melting and possible vaporization of the PFC materials. Possible burnout of cooling tubes as well as introduction of impurities into the plasma must be avoided². Plasma interactions with PFC have been studied for years both theoretically and experimentally^{1,3-5}. Several numerical codes have been developed and compared with available experimental results⁵. The problem is largely complex involving different scientific areas and has a dynamic evolution. The simultaneous solution of different dynamic and coupled models as well as the solution of moving boundaries is required. The fundamental processes can be grouped as follows: a) thermal heat conduction in divertor components while material melts and vaporizes. Erosion can also be calculated in this phase b) vapor plasma magnetohydrodynamics (MHD) in the vapor cloud formed above material surface undergoing erosion, and c) the radiation transport of the photons created by the plasma particles slowing down into the vapor plasma cloud.

HEIGHTS-PIC package is being developed to solve a multidimensional plasma evolution after an intense energy deposition from plasma instabilities impinged on the PFC. The purpose of such package is to verify other HEIGHTS models and to develop another path for the solution of the integrated and complicated physical models involved. The plasma disruption has been numerically interpreted as beam of specified energy and spatial characteristics (shapes) applied along the time specified. Specific information about the sample PIC movements as well as of the upper vapor front can be tracked and visualized. The heat conduction part is solved with an implicit method. Detailed physical models of plasma-solid-liquid-vapor interactions with the presence of a strong inclined magnetic field have been developed in a self-consistent model coupled with radiation MHD models. Once the melted material becomes vaporized and starts expanding, plasma interacts with vapor resulting in photon radiation due to the slowing down of the particles.

Part of the radiation power is absorbed by the divertor/wall structure, but the presence of the vapor acts as a screen to the incoming energy flux. HEIGHTS-PIC can predict the macroscopic erosion solving the four moving boundaries. The analysis is performed for plasma parameters and conditions in ITER-like device for carbon-based divertor as PFC.

Plasma ELM/disruption modeling is presented and explained as well as the new approach proposed into the PIC technique. Results for giant ELM simulations are presented and discussed. The paper will be concluded with a brief discussion of future developments and research expansion needed to improve this new model.

II. PARTICLE-IN-CELL TECHNIQUE AND MODEL SUMMARY

The Particle-In-Cell (PIC) method was initially developed at Los Alamos in 1955 to address complex problems in fluid dynamic⁶⁻⁷. The method (later applied successfully in astro-dynamics to predict the evolution of the arms of the galaxies) is very useful when applied to multidimensional problems as well as when the fluid faces large distortions, colliding surfaces, or shocks of various types. The method uses the Eulerian and Lagrangian approaches at the same time in attempt to combine some of the best features of both. Since its introduction, significant improvements have been proposed and solutions to adapt the technique to plasma where it has shown to be very flexible and useful⁸⁻⁹. The “classical” PIC method is a partially Lagrangian description of the fluid. To each particle mass and a position are attributed. The “full particle” PIC formulations¹⁰⁻¹² are a fully Lagrangian description of the fluid. To each particle all the properties of the fluid are attributed including momentum and energy. Diffusion due to the presence of the B field needs also to be considered and incorporated into the particle motion. In the HEIGHTS-PIC simulation package a new approach is proposed different from the most known techniques used and is implemented in order to overcome some of the major problems like strong numerical diffusion, choice of the shape function or initial loading of the particles. HEIGHTS-PIC is essentially a “full-particle” representation being the momentum and energy Lagrangian variables. The position of the expanding vapor front is monitored constantly and compared to the original position of birth of the particles. A fixed grid is used for the Eulerian frame while an adapted one is used in to the Lagrangian step. Since the grid is used as an updated Lagrangian frame, the nonlinear convection term associated with Eulerian formulations does not appear. With the use of maps between material points and the grid, the advantages of both Eulerian and Lagrangian schemes are utilized. The vapor-plasma cloud is highly

dynamic and collisional and develops with an increasing number of particles incoming from the divertor surface. After the material starts vaporizing, the area of interest is enriched by the formation of new particles of vapor that tend to interact with the existing ones as well as the plasma. The incoming disruption energy is numerically interpreted as a beam of energy of specific shape: exponential, Gaussian or homogeneous. Energy is deposited onto the divertor proportionally to the path and speed of the ions subjected to the magnetic field **path**. While the heat conduction equation is solved to find the new temperatures of the material, the time step applied is very small (nanoseconds) and it is assumed that the new characteristics of the particles inside the cells are homogeneous throughout the cells themselves. As the system produces enough new real particles to produce a new larger sample one, this is added to the closest cell to the divertor surface according to the position of birth. The position of all sample particles is constantly known throughout the mesh and the solution of the Eulerian and Lagrangian steps. Each value of pressure, velocity, energy, density and temperature associated with the center of the cell is also known at each time step: these values are averaged with the bordering cells (in x direction and y direction) in order to significantly reduce numerical diffusion processes as well as numerical instabilities. The radiation transport in HEIGHTS-PIC is solved at each time step and provides better understanding of the plasma evolution process especially when radiation energy and vapor screening effect become significant towards the divertor. Part of the energy is radiated away towards other PFC while plasma energy is transmitted to the divertor surface only indirectly through photon radiation transport through the cloud controlling the final erosion of the divertor surface¹³. Photon radiation is composed of two different fluxes: continuum radiation and line radiation. Opacity and emissivity data are provided through extensive calculated tables covering a wide range of vapor density and temperatures¹⁴.

II.A. Plasma – Target Interaction

As the direct energy from the impinging plasma starts vaporizing the target material, the produced vapor will expand and start interacting with the incoming plasma. The deposition of plasma energy will then produce intense bulk vapor heating with subsequent vapor ionization. The ionized vapor will start interacting with the inclined magnetic field that will limit the expansion of the vapor. The ions will only move along the magnetic lines. In this condition further heating of the surface is due only to vapor thermal radiation and thermal conduction. The expansion of the vapor into vacuum is then determined by solving the MHD equations for conservation of mass, momentum and energy¹³:

$$\begin{aligned} \frac{\partial \rho}{\partial t} + \nabla \cdot (\rho \vec{V}) &= 0 \\ \rho \frac{\partial \vec{V}}{\partial t} + \nabla(P) &= 0 \\ \frac{\partial E}{\partial t} + \nabla(E \cdot \vec{V}) + P \nabla \cdot (\vec{V}) &= \nabla \cdot (K \nabla T) + \nabla \cdot Q_r + \nabla \cdot Q_b \end{aligned} \quad (1)$$

where ρ is the density, \vec{V} is the vapor velocity, P the pressure, E the energy, K the vapor conductivity, Q_b is the incident particle flux from the incoming plasma and Q_r is the radiation flux. The vapor plasma once it is ionized moves freely along the inclined magnetic field lines. The equation describing the vapor motion in a magnetic field is given by:

$$\rho \frac{\partial \vec{V}}{\partial t} = -\nabla P + \vec{J} \times \vec{B} \quad (2)$$

The magnetic force $\vec{J} \times \vec{B}$ acts as a retarding force for the expanding vapor with important consequences towards the final and total erosion of the plate. The perpendicular component to the B field of the force is predominant. Two parts compose the magnetic force: $F_{magnetic}$ or magnetic pressure force and $F_{curvature}$ due to the curvature of the magnetic field. The current density is given by:

$$\vec{J} = \frac{1}{\mu_0} \nabla \times \vec{B} \quad (3)$$

The magnetic diffusion in the vapor cloud needs to be considered in the solution of the MHD equation¹. The variation along time of the magnetic field can be calculated with:

$$\frac{\partial \vec{B}}{\partial t} = -\frac{1}{\mu_0} \nabla \times (\varepsilon + \vec{V} \times \vec{B}) \quad (4)$$

where ε is the induced electric field and can be calculated as $\varepsilon = \vec{J} / \sigma$. The vapor conductivity σ for weakly ionized plasma is directly proportional to the vapor plasma collision time τ and density n_e and inversely proportional to the mass of the electron.

II.B. Radiation Transport

After enough vapor has accumulated in front of the divertor plate, the impinging plasma particles will be totally stopped by the vapor cloud with residual heating and ionization of the cloud itself. Photon radiation by the vapor cloud is then emitted due to the continuous vapor

heating process. At this point plasma energy is transmitted to the divertor surface only indirectly through photon radiation determining the final erosion rate. Radiation is composed by two different fluxes: continuum radiation and line radiation. Opacity and emissivity data are provided through tables covering a wide range of vapor density and temperatures. They have been calculated using the HEIGHTS atomic physics package¹⁴.

III. DIVERTOR GEOMETRY AND COMPUTATIONAL SETUP

The basic geometry for the divertor used for the simulations is the ITER design submitted to the ITER parties in the “ITER-FEAT outline design”¹⁵. The current design assumes carbon-based material for the vertical inner and outer divertor. For our calculation graphite properties were assumed. The strike point was assumed at the $x = 0$ axis (Fig. 1) with an inclined B field with respect to the divertor of 5° . The value of the B field was chosen to be 50 kGauss. The energy and particle losses across the magnetic field are diffusive processes with a diffusion coefficient assumed about 10 times larger than the normal operation and equal to $D_{\perp} = 5 \text{ m}^2 / \text{s}$ (Ref. 16). The poloidal direction of the B field is along x axis while the toroidal magnetic field is in z direction which is into the page (Fig. 1).

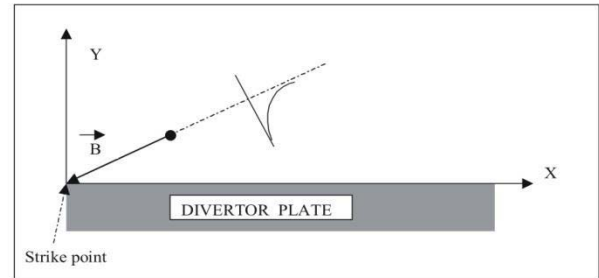


Fig 1. Schematic illustration of ELM modeling

The spatial distribution of the ELM plasma impact is modeled assuming an exponential shape¹⁶⁻¹⁷. During an ELM only a fraction of the tokamak plasma energy escapes to the SOL and then to the divertor. For the simulations giant ELM conditions were considered. A $Q_{ELM} = 10\% Q_0$ ($\eta = 0.1$) corresponds to a total of 12.6 MJ of total ELM energy (10% of pedestal energy). This distribution keeps the maximum power density carried by the plasma at midplane equal to $4.60 \text{ MW} / \text{cm}^2$ (corresponding at $0.460 \text{ MW} / \text{cm}^2$ at the strike point) with an e-fold length of the plasma power profile above the divertor plate of 6.7 cm for 0.1 ms. The initial temperature of the ELM plasma was taken as 3.5 keV. The major radius in ITER-like geometry is equal to 6.5 m. Several cases have been studied with an increasing number of sample particles representing the bulk of the

plasma. In particular, the ratio of real particles per sample one has been set to $0.25 \times 10^{16} \# / N_{sample}$ and cases where run also for half and double this value. The ELM modeling includes the interaction with the divertor solid target, vaporized gas, and divertor plasma in magnetic field configuration. Several blocks constitute the HEIGHTS-PIC package including heat conduction, divertor surface vaporization and particle generation, plasma material interaction and MHD models. The MHD block (Eulerian and Lagrangian part) integrates the plasma hydrodynamic evolution, magnetic diffusion, heat conduction, and radiation transport.

IV. SIMULATION RESULTS & BENCHMARKING

The PIC model of the ELM effect on the divertor using the ITER-like geometry confirmed previous analysis about the erosion depth and profile^{4,16,18}. The complex behavior of plasma with an inclined magnetic

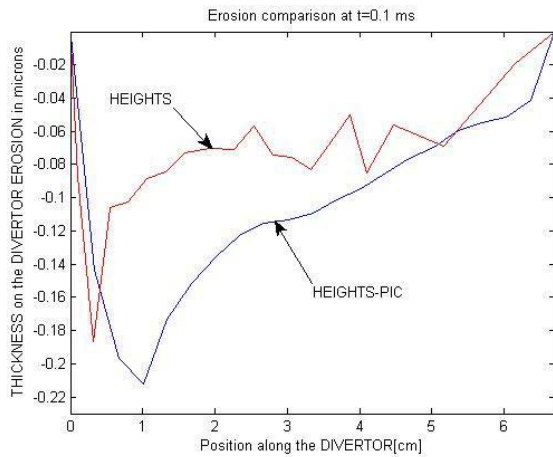


Fig 2. Divertor erosion profile comparison after a giant ELM impact of 0.1 ms duration.

field strongly influences the capacity of the vapor to shield and reduce the erosion on the surface. The interplay of the three main phenomena (impact of plasma on the surface with formation of a vapor cloud, radiation from the vapor cloud, and heat conduction into the divertor plate) exerts different roles according to the impact duration of the ELM and disruption. Figure 2 shows the final divertor surface erosion profile and comparison with the HEIGHTS results. The maximum erosion is in the same order of magnitude and with very close values to the ones predicted by HEIGHTS. The shape of the final erosion is also very similar and less characterized by local numerical perturbations. During the impact duration of 0.1 ms, the impinging plasma initiates a strong surface vaporization. Most of the initial impact energy is spent in further eroding the carbon-based material close to the strike point. As vapor starts forming and becomes more

dense the deceleration of the plasma particles interacting with the vapor, reduces the effective energy reaching the divertor (Fig. 3). The net erosion rate is then reduced with slight broadening effect towards the rest of the plate. As the vapor shields becomes more efficient in the screening effect, the broadening will become wider and wider since most of the energy directly impinging the plate mainly

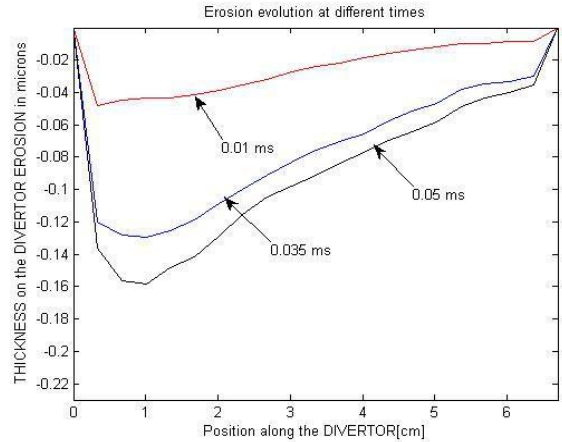


Fig 3. Spatial evolution of divertor erosion profile after a giant ELM impact at different times.

comes from the photons radiation and transport through less dense areas. The vapor-plasma cloud formed can reach temperatures up to tens of eV (Fig. 4) and shields very efficiently close to the strike point the surface from the incoming ELM particles due to insufficient time for the vapor motion and transport.

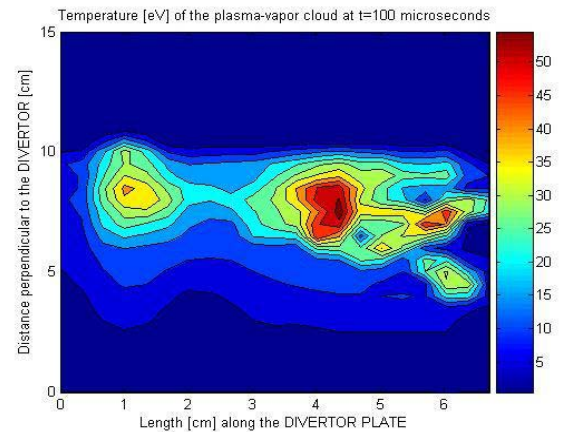


Fig 4. Temperature distribution of the vapor-plasma cloud above the divertor at t = 0.1 ms.

The incident ELM energy is used for the vaporization process, heating of the vapor plasma, and then significant re-radiation from the vapor cloud to nearby locations. Changing the ratio of real particles to sample ones (for example to 1/2 of the simulation previously described) showed very small differences both in the erosion profile

and in the final temperature snapshot. Those differences are in the order of 5% to 10 %. In Figure 4, the vapor cloud is expanded at a distance of 5 to 10 cm normal to the divertor plate for 0.1 ms. The peaks of temperature are determined by the different vapor screening effect according to location and follow the major erosion profile provoked onto the divertor plate.

V. CONCLUSIONS

ELMs and disruptions represent a serious problem for plasma facing components during normal and abnormal operations in tokamak devices. To evaluate the characteristics of this problem, a particle-in-cell (PIC) method is being developed. The models in HEIGHTS-PIC provide through a novel use of the PIC technique a detailed picture of the plasma-vapor interaction and evolution during ELM events. Detailed plasma energy deposition model, thermal conduction, melting, evaporation and vapor expansion are included. The interaction of plasma with expanding vapor is examined for plasma energy transient deposition up to 0.1ms. HEIGHTS-PIC was benchmarked against several other models in the well benchmarked Eulerian and Lagrangian original HEIGHTS package and showed a good agreement in the simulation of the plasma behavior during ELMs events and the overall divertor erosion profiles. Future work will extend the existing models improving the radiation transport part with the use of Monte-Carlo methods and parallelizing the structure of the code. The flexibility of PIC methods will be used in adapting complicated divertor/wall structures as well as nearby components to assess in detail the damage to these components as well. Additionally, more analysis for various ELMs and disruptions conditions will be analyzed and studied.

ACKNOWLEDGMENTS

This work is supported by the US Department of Energy, Office of Fusion Energy Sciences.

REFERENCES

1. A., HASSANEIN, T., SIZYUK (2008). "Comprehensive simulation of vertical plasma instability events and their serious damage to ITER plasma facing components." *J. of Nuclear Fusion*, **48**, 115008.
2. A. HASSANEIN et Al.(2010),"Impact of various plasma instabilities on reliability and performance of tokamak fusion devices.", *Fusion Eng. Des.*,**85**:1331-1335.
3. A.S., KUKUSHKIN, H.D., PACHER et al. (2003). "Divertor issues on ITER and extrapolation to reactors." *Fusion Engin. and Des.* **65**(3): 355-366.
4. A., HASSANEIN, T., SIZYUK et al. (2009). "Integrated simulation of plasma surface interaction during edge localized modes and disruptions: Self-consistent approach." *Journal of Nuclear Mat.* **390-91**: 777-780.
5. G., FEDERICI, A. LOARTE, et al. (2003). "Assessment of erosion of the ITER divertor targets during type I ELMs". *Plasma Physics and Controlled Fusion* **45**(9):1523-1547.
6. F.H., HARLOW(1955)."Machine calculation method for hydrodynamics problems". Los Alamos Scientific Laboratory Report LAMS-1956.
7. M.W. EVANS and F.H. HARLOW (1957)."The Particle-in-Cell Method for hydrodynamic calculations." Los Alamos Scientific L. LA-2139.
8. C.K. BIRDSALL and D. FUSS(1969)."Clouds-in-clouds, clouds-in-cell physics for many-body plasma simulations",*J. Comp. Phys.*,**3**,494.
9. C.K. BIRDSALL, A.B., LANGDON and H. OKUDU (1970)."Finite-size particle physics applied to plasma simulation", *Meth. Comp. Phys.*, **9**,242.
10. J.U. BRACKBILL and W.E. PRACHT (1973)." An Implicit Almost-Lagrangian Algorithm for Magnetohydrodynamics." *J. Comput. Phys.* **13**:455.
11. J.U. BRACKBILL and H.M. RUPPEL (1986). "FLIP - A method for adaptively zoned, Particle-in-Cell calculation of fluid-flows in 2 dimensions." *Journal of Computational Physics* **65**(2): 314-343.
12. J.U., BRACKBILL, D. B., KOTHE et al. (1988). "FLIP-A low-dissipation, Particle-in-Cell method for fluid-flow." *Computer Physics Commun.* **48**(1):25-38
13. A. HASSANEIN and I. KONKASHBAEV (1994)."Modeling plasma/material interactions during tokamak disruption",*ANL/FPP/TM-271*.
14. V., MOROZOV, V., TOLKACH and A. HASSANEIN ,(2004) "Calculation of Tin atomic data and plasma properties",*Argonne National Lab Report,ANL-ET-04/24 Argonne, Illinois*.
15. R., AYMAR (2001). "ITER R&D: Executive summary: Design overview." *Fusion Engineering and Design* **55**(2-3): 107-118.
16. A. HASSANEIN and I. KONKASHBAEV (2003). "Comprehensive modeling of ELMs and their effect on plasma-facing surfaces during normal tokamak operation." *Journal of Nuclear Mat.* **313**: 664-669
17. R.A.PITTS et Al.,(2007)"ELM Transport in the JET scrape-off layer", *J. of Nuclear Fusion*,**47**,1437-1448.
18. V., SIZYUK, A., HASSANEIN (2010)."Damage to nearby divertor components of ITER-like devices during giant ELMs and disruptions", *J. of Nuclear Fusion* ,**50**,115004.